

Ab initio study of superconducting hexagonal Be₂Li under pressureIon Errea,^{1,2} Miguel Martínez-Canales,^{1,2} and Aitor Bergara^{1,2,3}¹*Materia Kondentsatuaren Fisika Saila, Zientzia eta Teknologia Fakultatea, Euskal Herriko Unibertsitatea, 644 Postakutxatila, 48080 Bilbo, Basque Country, Spain*²*Donostia International Physics Center (DIPC), Paseo de Manuel Lardizabal 4, 20018 Donostia, Basque Country, Spain*³*Centro Mixto CSIC-UPV/EHU, 1072 Posta kutxatila, E-20080 Donostia, Basque Country, Spain*

(Received 29 September 2008; published 5 November 2008)

Following the recent interest on lithium alloys under pressure, we present first-principles calculations of the electronic band structure and lattice dynamics for the MgB₂-like layered Be₂Li at 80 GPa. Under pressure, the increasing electronic localization reduces the effective dimensionality of Be₂Li, showing both two-dimensional and one-dimensional conducting electronic channels. The numerical results reveal the presence of an ultrasoft strongly anharmonic B_{2g} phonon mode associated to the atomic buckling in the layers, which shows a high electron-phonon interaction near the zone center and (besides the moderately coupled E_{2g} in-plane and A_{1g} interlayer Be modes) is responsible for a predicted superconducting transition around 2.5 K.

DOI: [10.1103/PhysRevB.78.172501](https://doi.org/10.1103/PhysRevB.78.172501)

PACS number(s): 74.70.Ad, 74.62.Fj

It is well known that physical properties of materials can be strongly modified by pressure so that it can be effectively used to tune both structural and electronic properties. Under compression, not only do complex structures arise but superconductivity can also be enhanced.^{1,2} Even simple metals break conventional wisdom and facilitate the stability of open structures,^{3–9} which are driven by the induced anisotropy of the chemical bonding associated to the increasing electronic hybridization. Furthermore, this correlation between structural transitions and the increasing electronic localization¹⁰ usually implies a deep modification of the phonon spectrum which might enhance the electron-phonon coupling responsible for the superconducting transition,^{11–15} thus posing a challenge to the conventional Matthias' rule.¹⁶

The discovery of MgB₂ (Ref. 17) probed the success of light element alloys in order to enhance the superconducting T_c . Actually, its hexagonal layered structure is shared by a large class of alloys with relatively high superconducting transition temperatures, such as CaSi₂,¹⁸ ternary silicides,^{19,20} and alkaline-earth intercalated graphites.^{21,22} Additionally, as has been recently observed in CaLi₂,^{23,24} pressure seems to favor highly anisotropic superconducting structures when light elements are alloyed. Furthermore, Feng *et al.*²⁵ recently predicted that, although at normal conditions Li and Be are immiscible, under pressure Be₂Li adopts a MgB₂-like structure with $P6/mmm$ symmetry.²⁵ As shown in Fig. 1, similarly to MgB₂, its lattice is formed by alternate graphene layers of Be and Li atoms^{26,27} that are intercalated with Be atoms sitting at the center of each underlying hexagon. Considering that the high T_c in MgB₂ (Ref. 17) is related to the giant anharmonicity of the E_{2g} in-plane phonons, which are associated to the coexistence of large electron-phonon coupling and small Fermi energies,²⁸ it is sensible to wonder whether such features also arise for the hexagonal Be₂Li. Additionally, as Be₂Li combines the two lightest metallic atoms, it is expected to have a high Debye temperature, which also might contribute to enhance T_c . Although hexagonal Be₂Li is predicted to be thermodynamically favored above 15 GPa,²⁵ our calculations indicate that just above 70 GPa it becomes dynamically stable. With these considerations in mind, this Brief Report presents an *ab initio* analy-

sis of the microscopic properties of the hexagonal Be₂Li at 80 GPa in order to identify anomalous features in both vibrational and electronic spectra inducing the superconducting transition.

The electronic properties have been calculated within the density-functional theory (DFT) (Refs. 29 and 30) framework, while lattice dynamics and the electron-phonon coupling have been computed using density-functional perturbation theory (DFPT) (Ref. 31) as implemented in the QUANTUM-ESPRESSO (PWSCF) (Ref. 32) package. In order to approximate the exchange-correlation functional, the local-density approximation (LDA) within Perdew-Zunger³³ parametrization has been used. Both 1s electrons of Li and Be

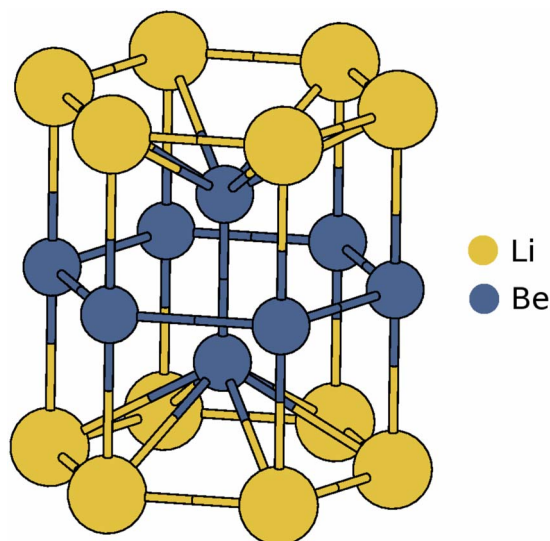


FIG. 1. (Color online) From the structural point of view, at high pressure Be₂Li has been predicted (Ref. 25) to be very similar to MgB₂, with alternate graphene layers of Be and Li atoms intercalated with Be atoms sitting at the center of each underlying hexagon with $P6/mmm$ symmetry. The cell parameters of the relaxed structure at 80 GPa are $a=b=3.133\ 57$ and $c=3.893\ 50$ Å. Although predicted to be thermodynamically favored above 15 GPa, it becomes dynamically stable above 70 GPa.

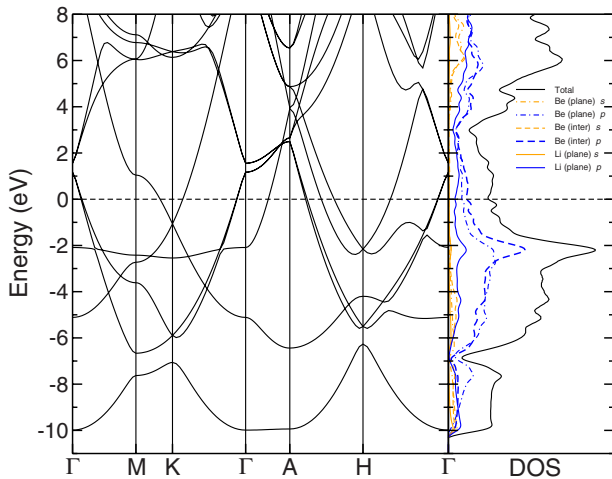


FIG. 2. (Color online) Band structure and decomposed DOS of hexagonal Be_2Li at 80 GPa. Fermi level is depicted with a dashed line. In spite of the applied high pressure, the band structure shows highly anisotropic features mainly induced by its layered atomic geometry, which are almost unaffected by pressure. Both 1D- and 2D-like bands are distinguished, which is also confirmed in the DOS, where a 1D-like smoothed singularity and 2D steplike contributions can be observed.

are treated as core electrons by the norm-conserving pseudopotentials that include nonlinear core corrections. The desired convergence for the used plane-wave basis has been achieved with a 34 Ry cutoff. The phonon-dispersion curves have been calculated from the interatomic force-constant (IFC) matrix, which has been Fourier interpolated from a $4 \times 4 \times 4$ grid after its convergence has been checked by performing a denser interpolation on a $6 \times 6 \times 6$ grid. In order to integrate over the Brillouin zone (BZ), a Γ -centered $20 \times 20 \times 20$ mesh³⁴ has been enough to reach convergence for most calculations. On the contrary, converging the double delta needed for the electron-phonon interaction coefficients has required a finer $60 \times 60 \times 60$ grid. Calculations have been performed after a full cell relaxation.

Similar to MgB_2 , the layered structure of Be_2Li favors the electronic localization in the atomic planes. As appreciated in Fig. 2, its electronic bands also reflect the anisotropy of the structure and, interestingly, address contributions to conductivity coming from the interplay of two-dimensional (2D) and even one-dimensional (1D) electronic features. Some bands are quasi-2D, being free-electron-like in the layers and almost flat along its perpendicular direction (Γ -A), which is also confirmed by the electronic density of states (DOS) which shows the characteristic steplike feature associated to 2D systems. Additionally, at around 2 eV below the Fermi level the presence of a 1D-like band is also remarkable, which is highly dispersive and parabolic along Γ -A but becomes almost flat in the Γ -M-K plane. This band explains the large peak in the DOS at 2 eV below the Fermi level, corresponding to a smoothed 1D-like singularity. As confirmed by the observed peaks in the decomposed DOS (Fig. 2) of p -like states associated to Li and interlayer Be, this 1D conduction channel is mainly related to the electrons localized at the center of the hexagons in the Li layers that conduct along

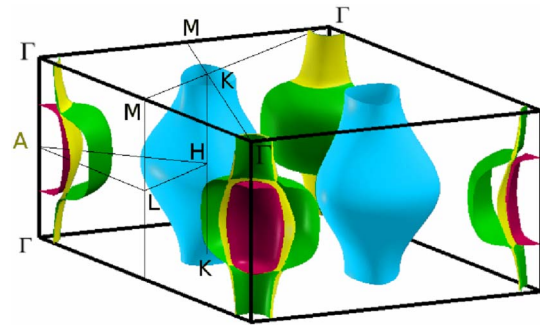


FIG. 3. (Color online) The Fermi surface of Be_2Li at 80 GPa is made of four distinctive sheets and evidences the interplay of 2D and even 1D electronic features. Note the effects of anticrossing. Meanwhile, the intersection between the two cylinders is depicted with color change.

its perpendicular direction through interlayer Be atoms. Although electrons moving in Be planes are free-electron-like, with a maximum electronic localization³⁵ value of 0.7, the electron localization function (ELF) reaches 0.9 at the center of Li hexagons, confirming the strong electronic localization in the Li planes. This difference can be associated to their different atomic radius. Since the Li atomic radius is larger than the Be one, as pressure is raised, Li cores start to overlap expelling the electrons in the plane into the center of the hexagons. In order to characterize the effect of these interlayer Be atoms, the band structure has been recalculated, removing them but keeping the same structure. Analyzing differences in the charge density, we conclude that a large amount of the electronic charge associated to interlayer Be goes to the center of both surrounding planes, but the most striking feature is that by removing interlayer Be atoms the flat 1D band is no longer occupied and the above-mentioned electronic localization completely disappears, confirming the main role of interlayer Be atoms favoring the occupation of this 1D conduction channel. This feature is in stark contrast to MgB_2 , where the interplanar Mg atom is completely ionized,³⁶ just acting as a reservoir of charge for the B planes without playing any important role, so that this 1D band becomes completely unoccupied, decreasing the Fermi energy of the holes in σ bands.

As shown in Fig. 3, the above-mentioned main features also characterize its Fermi surface, which is made of four distinctive bands. A flattened region perpendicular to Γ -A evidences 1D electronic behavior and, similar to the Fermi surface of MgB_2 ,³⁷ two cylinders that are aligned along Γ -A and associated to the 2D σ -like bands are observed. A thorough symmetry analysis reveals that the first cylinder and flattened band share the same symmetry so that anticrossing occurs between them. Considering that the second cylinder has different symmetry, it intersects the other sheet. This analysis reinforces the idea of 1D behavior, which is absent in MgB_2 . Finally, another quasicylindrical sheet (on blue) along K-H, linked with electronic states that are mainly localized in the atomic planes, is also appreciated.

Considering the structural similarities of Be_2Li with MgB_2 , it is sensible to wonder if they also have similar lattice dynamics and electron-phonon coupling (see Fig. 4). In

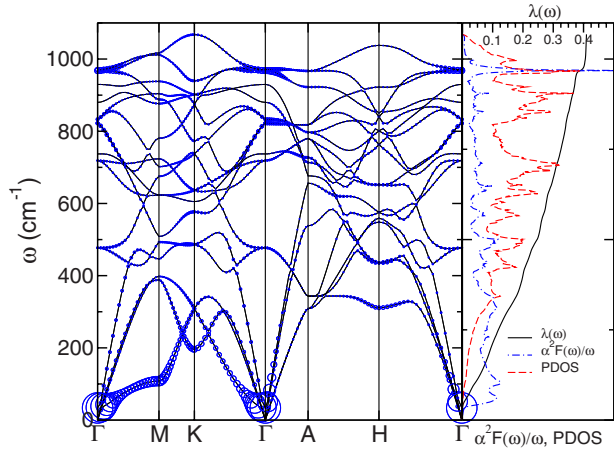


FIG. 4. (Color online) (Left panel) The calculated phonon dispersion of Be_2Li at 80 GPa. The area of each circle is proportional to the partial electron-phonon coupling, $\lambda_{\mathbf{q}\nu}$. The usual electron-phonon parameter, λ , is $\sum_{\mathbf{q}\nu} \lambda_{\mathbf{q}\nu}$. (Right panel) The phonon spectral function $\alpha^2 F(\omega)/\omega$ and the electron-phonon integral, $\lambda(\omega) = 2 \int_0^\omega \alpha^2 F(\omega')/\omega' d\omega'$, are compared to the PDOS.

MgB_2 the E_{2g} mode softens at Γ , which is very strongly coupled to the planar B σ bands. Its high anharmonicity is directly related to the large electron-phonon coupling.²⁸ The unit cell of Be_2Li includes one hexagonal layer for each atom type; therefore, it shows two E_{2g} modes: one associated to atomic stretching in Be planes with $\omega = 970 \text{ cm}^{-1}$ at Γ and another one corresponding to Li layers with 822 cm^{-1} . This frequency difference indicates that the atomic repulsion is higher in Be planes. Contrary to MgB_2 , both modes are highly harmonic with an almost flat dispersion. Fitting the energy, as a function of the displacement of the atoms according to these modes, to $E(u) = au^2 + bu^4$, the obtained anharmonic ratio b/a^2 for the Be E_{2g} mode is 0.04 eV^{-1} , while for Li E_{2g} reaches 0.01, which is both negligible compared to MgB_2 , with an anharmonic ratio of about 8. In order to characterize this difference we have analyzed the modification in the electronic bands when the lattice is distorted according to these E_{2g} modes. As shown in Fig. 5(a), these distortions split the σ -like bands but, contrary to MgB_2 , this is not enough to fully drop any of them below the Fermi energy. Therefore, typical atomic displacements (according to the E_{2g} modes) do not increase the DOS at the Fermi level as much as in MgB_2 , and their associated electron-phonon coupling is not so high. Although among the E_{2g} modes the one associated to Be planes has the largest partial electron-phonon interaction, the almost degenerate A_{1g} mode with $\omega = 968 \text{ cm}^{-1}$ at Γ presents an even larger $\lambda_{\mathbf{q}\nu}$. This mode involves a motion of the interlayer Be atoms along z . Considering lattice distortions according to the A_{1g} mode, main modifications in the band structure are observed when interlayer Be atoms approach Be planes [Fig. 5(b)]: the σ -like band drops below the Fermi energy just at Γ , although not along the whole Γ -A line. Its anharmonic ratio is 0.14 eV^{-1} . In contrast to Be_2Li , in MgB_2 the 1D-like conduction channel is completely unoccupied and the electronic interaction with Mg atoms is small, so that this mode becomes inefficient.

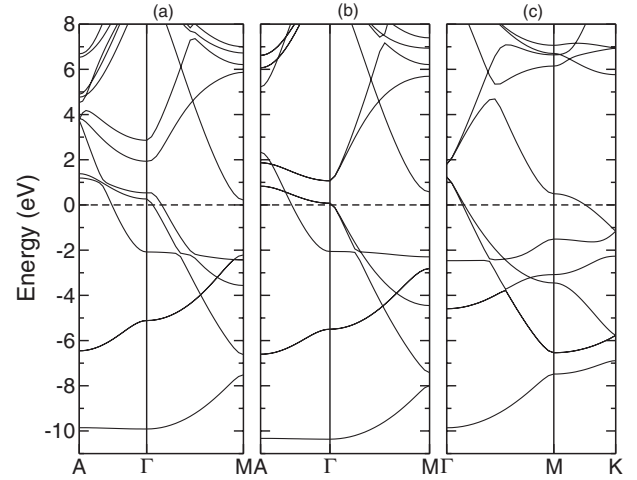


FIG. 5. Band structure of Be_2Li at 80 GPa when the lattice is distorted according to (a) Be E_{2g} mode along A- Γ -M, (b) A_{1g} mode with the atoms displaced toward the Be plane along A- Γ -M, and (c) B_{2g} mode along Γ -M-K. The considered atomic displacements range between 0.16 and 0.2 Å.

Even more interestingly, in Fig. 4, it is clearly appreciated that the largest partial electron-phonon coupling is associated to the ultrasoft optical mode of B_{2g} symmetry with 34 cm^{-1} at Γ , which consists of a zig-zag out-of-plane motion of the atoms in both Li and Be planes. Fitting the energy as a function of atomic displacement for this mode shows a giant anharmonic ratio of 44 eV^{-1} , and below 70 GPa it becomes unstable around Γ , favoring the corrugation in both atomic layers. Actually, the observed softening and anharmonic behavior of this mode is directly related to the coupling between simultaneous atomic displacements in both Li and Be planes as it becomes harmonic when distortions of different planes are independently considered. As shown in Fig. 5(c), typical distortions according to the B_{2g} mode increase the dispersion in the 1D channel, so that the band gap is considerably decreased at M, increasing the DOS that induces the observed anharmonicity and softening. Interestingly, a very similar strongly coupled soft mode has been proposed in other structurally related compounds, such as CaAlSi (Refs. 38 and 39) and compressed CaSi_2 ,⁴⁰ as being responsible for their relatively high superconducting transition temperatures at 7.8 and 14 K, respectively. Actually, recent experiments on CaAlSi (Ref. 41) have confirmed this picture.

In the right panel of Fig. 4 the calculated Eliashberg function $\alpha^2 F(\omega)$ divided by ω is compared to the phonon density of states (PDOS). Deltalike peaks around 970 cm^{-1} in both the spectral function and the PDOS are a direct consequence of the relevant phonon linewidth, $\gamma_{\mathbf{q}\nu}$, of the Einstein-type A_{1g} and Be E_{2g} modes: 5.3 and 2.8 meV at Γ , respectively. However, at low frequencies the spectral function becomes uncorrelated with the PDOS, and the main contribution is associated to the soft phonon. Although its phonon linewidth is not high [0.2 meV at Γ and similar to the measured linewidth of the soft mode in superconducting CaAlSi (Ref. 41)], the low frequency of this soft mode enhances its coupling to the electronic system, $\lambda_{\mathbf{q}\nu}$, and favors the superconducting transition. The total λ of Be_2Li at 80 GPa obtained from the

computed isotropic Eliashberg function is 0.41. Using the McMillan⁴² expression for T_c with the calculated logarithmic average frequency of 512 K and assuming $\mu^*=0.1$, we obtain $T_c=2.5$ K.

In conclusion, contrary to MgB₂, where superconductivity is driven by the strongly coupled high-energy phonon mode, but similar to CaAlSi (Refs. 38 and 39) and compressed CaSi₂,⁴⁰ the predicted superconducting transition in Be₂Li is mainly originated by pressure-induced structural instability, leading to the presence of a soft mode related to the atomic planar buckling. Furthermore, considering the electronic and dynamic features of Be₂Li at 80 GPa analyzed above, both anharmonic corrections^{28,43} associated to the soft mode and

the anisotropic⁴⁴ framework associated to Eliashberg theory are expected to enhance the predicted T_c .

The research presented herein was funded by the Spanish Ministry of Education and Science under Project No. BFM2003-04428. I.E. would like to thank the Basque Department of Education, Universities and Research for financial help. M.M.C. is also thankful to the Spanish Ministry of Education and Science for economic support under Grant No. BES-2005-8057. Finally, the authors are also thankful to SGI-IZO SGIker UPV EHU for the allocation of computational resources, as these have made the present work a reality.

-
- ¹J. S. Schilling, *Treatise on High Temperature Superconductivity* (Springer-Verlag, Hamburg, 2006).
- ²N. W. Ashcroft, *Nature (London)* **419**, 569 (2002).
- ³J. B. Neaton and N. W. Ashcroft, *Nature (London)* **400**, 141 (1999).
- ⁴M. Hanfland, K. Syassen, N. E. Christensen, and D. L. Novikov, *Nature (London)* **408**, 174 (2000).
- ⁵J. B. Neaton and N. W. Ashcroft, *Phys. Rev. Lett.* **86**, 2830 (2001).
- ⁶M. I. McMahon, S. Rekhi, and R. J. Nelmes, *Phys. Rev. Lett.* **87**, 055501 (2001).
- ⁷M. I. McMahon, R. J. Nelmes, and S. Rekhi, *Phys. Rev. Lett.* **87**, 255502 (2001).
- ⁸R. J. Nelmes, M. I. McMahon, J. S. Loveday, and S. Rekhi, *Phys. Rev. Lett.* **88**, 155503 (2002).
- ⁹M. Hanfland, I. Loa, and K. Syassen, *Phys. Rev. B* **65**, 184109 (2002).
- ¹⁰J. S. Tse, Y. Yao, and Y. Ma, *J. Phys.: Condens. Matter* **19**, 425208 (2007).
- ¹¹V. V. Struzhkin, M. I. Eremets, W. Gan, H. K. Mao, and R. J. Hemley, *Science* **298**, 1213 (2002).
- ¹²K. Shimizu, H. Ishikawa, D. Takao, T. Yagi, and K. Amaya, *Nature (London)* **419**, 597 (2002).
- ¹³S. Deemyad and J. S. Schilling, *Phys. Rev. Lett.* **91**, 167001 (2003).
- ¹⁴T. Yabuuchi, T. Matsuoka, Y. Nakamoto, and K. Shimizu, *J. Phys. Soc. Jpn.* **75**, 083703 (2006).
- ¹⁵J. J. Hamlin, V. G. Tissen, and J. S. Schilling, *Phys. Rev. B* **73**, 094522 (2006).
- ¹⁶B. T. Matthias, *Phys. Rev.* **97**, 74 (1955).
- ¹⁷J. Nagamatsu, N. Nakagawa, T. Muranaka, Y. Zenitani, and J. Akimitsu, *Nature (London)* **410**, 63 (2001).
- ¹⁸S. Sanfilippo, H. Elsinger, M. Núñez-Regueiro, O. Laborde, S. LeFloch, M. Affronte, G. L. Olcese, and A. Palenzona, *Phys. Rev. B* **61**, R3800 (2000).
- ¹⁹M. Imai, K. Nishida, T. Kimura, and H. Abe, *Appl. Phys. Lett.* **80**, 1019 (2002).
- ²⁰M. Imai, E. Abe, J. Ye, K. Nishida, T. Kimura, K. Honma, H. Abe, and H. Kitazawa, *Phys. Rev. Lett.* **87**, 077003 (2001).
- ²¹T. E. Weller, M. Ellerby, S. S. Saxena, R. P. Smith, and N. T. Skipper, *Nat. Phys.* **1**, 39 (2005).
- ²²N. Emery, C. Hérold, M. d'Astuto, V. Garcia, Ch. Bellin, J. F. Marêché, P. Lagrange, and G. Loupiau, *Phys. Rev. Lett.* **95**, 087003 (2005).
- ²³J. Feng, N. W. Ashcroft, and R. Hoffmann, *Phys. Rev. Lett.* **98**, 247002 (2007).
- ²⁴T. Matsuoka, M. Debessai, J. J. Hamlin, A. K. Gangopadhyay, J. S. Schilling, and K. Shimizu, *Phys. Rev. Lett.* **100**, 197003 (2008).
- ²⁵J. Feng, R. Hening, N. W. Ashcroft, and R. Hoffmann, *Nature (London)* **451**, 445 (2008).
- ²⁶A. Bergara, J. B. Neaton, and N. W. Ashcroft, *Phys. Rev. B* **62**, 8494 (2000).
- ²⁷A. Rodriguez-Prieto and A. Bergara, *Phys. Rev. B* **72**, 125406 (2005).
- ²⁸T. Yildirim *et al.*, *Phys. Rev. Lett.* **87**, 037001 (2001).
- ²⁹P. Hohenberg and W. Kohn, *Phys. Rev.* **136**, B864 (1964).
- ³⁰W. Kohn and L. J. Sham, *Phys. Rev.* **140**, A1133 (1965).
- ³¹S. Baroni, S. de Gironcoli, A. Dal Corso, and P. Giannozzi, *Rev. Mod. Phys.* **73**, 515 (2001).
- ³²S. Baroni *et al.* (<http://www.pwscf.org/>).
- ³³J. P. Perdew and A. Zunger, *Phys. Rev. B* **23**, 5048 (1981).
- ³⁴H. J. Monkhorst and J. D. Pack, *Phys. Rev. B* **13**, 5188 (1976).
- ³⁵A. D. Becke and K. E. Edgecombe, *J. Chem. Phys.* **92**, 5397 (1990).
- ³⁶J. M. An and W. E. Pickett, *Phys. Rev. Lett.* **86**, 4366 (2001).
- ³⁷H. J. Choi, D. Roundy, H. Sun, M. L. Cohen, and S. G. Louie, *Nature (London)* **418**, 758 (2002).
- ³⁸I. I. Mazin and D. A. Papaconstantopoulos, *Phys. Rev. B* **69**, 180512(R) (2004).
- ³⁹G. Q. Huang, L. F. Chen, M. Liu, and D. Y. Xing, *Phys. Rev. B* **69**, 064509 (2004).
- ⁴⁰G. Satta, G. Profeta, F. Bernardini, A. Continenza, and S. Massidda, *Phys. Rev. B* **64**, 104507 (2001).
- ⁴¹S. Kuroiwa, A. Q. R. Baron, T. Muranaka, R. Heid, K.-P. Bohnen, and J. Akimitsu, *Phys. Rev. B* **77**, 140503(R) (2008).
- ⁴²W. L. McMillan, *Phys. Rev.* **167**, 331 (1968).
- ⁴³V. H. Crespi and M. L. Cohen, *Phys. Rev. B* **48**, 398 (1993).
- ⁴⁴H. J. Choi, M. L. Cohen, and S. G. Louie, *Phys. Rev. B* **73**, 104520 (2006).